Photocatalytic oxidation in phenol removal using Ru/TiO$_2$ and Ru/Al$_2$O$_3$ catalysts

[1]* Syaifullah Muhammad, [2]Edy Saputra, [3]Shaobin Wang

[1]Department of Chemical Engineering, Faculty of Engineering, Syiah Kuala University, Darussalam, Banda Aceh 23111, Indonesia.
[2] Chemical Engineering Department, Riau University, Pekanbaru, Indonesia
[3] Chemical Engineering Deparment, Curtin University of Technology, Western, Australia.
**Coorresponding Author*: syaiful.muhammad@unsyiah.ac.id

Abstract

Ru/TiO$_2$ and Ru/Al$_2$O$_3$ catalyst have been synthesized using impregnation method followed by calcinations at temperature of 550 ^{0}C. The synthesized catalysts were characterized by XRD, SEM and EDS. Based on characterization result, the active phase of Ru in form of RuO$_2$ was well coated and dispersed on the support surface. The catalysts were then used in photocatalytic oxidation of phenol in the presence of peroxymonosulphte (PMS) as an oxidant and UV-light from Mercury lamp which is categorized as UV-C, with wave length in range of 200-280 nm. Both catalyst are effective for application of photocatalytic oxidation of phenol in the present PMS and UV. Further, activation of PMS for the production of sulphate radicals for phenol degradation in this study is generated by the interaction PMS-Catalyst and PMS-UV. The photocatalytic catalyst of Ru/TiO$_2$ and Ru/Al$_2$O$_3$ can increase the removal efficiency of 10-15%. The activity in phenol removal of Ru/TiO$_2$-PMS-UV is slightly higher than Ru/Al$_2$O$_3$-PMS-UV. Both catalysts also showed good performance in the second and third runs after regeneration for multiple uses. Kinetic studies showed that phenol oxidation on the catalysts, Ru/TiO$_2$ and Ru/Al$_2$O$_3$ in the present of PMS and UV follows the first order reaction.

Key words: photocatalytic oxidation, peroxymonosulphte, sulphate radicals phenol degradation

Introduction

Generally, the removal technique of pollutants from waste water using sunlight such as UV-light is called photolysis. In this process, wastewater solution is irradiated with UV to produce hydroxyl radicals which is playing as oxidant agent in the degradation of organic waste in the water.

Removal efficiency of these contaminants will be better with the addition of semi-conductors such as TiO$_2$, ZnO, Al$_2$O$_3$ and others. The semiconductor absorbs the UV radiation more efficiently than pollutants to produce active hydroxyl radicals. To date, TiO$_2$ photocatalyst has been the most widely used than other metal oxides such as ZnO, ZrO$_2$, SrO$_2$, CdS etc (Serpone *et al.,* 1995)

TiO$_2$ has been extensively used due to low cost, low toxicity, chemical and photochemical stability, high photocatalytic activity, and biocompatibility (Spadavecchia *et al.,* 2010; Zhang *et al.,* 2011). However, some drawback of TiO$_2$ such as the low quantum yield of TiO$_2$ for practical applications, only sensitive for visible light irradiation, exhibits a high refractive index and shows limited photoactivity, has been reported (Cong and Xu, 2011; Paola *et al.,* 2012; Grieken *et al.,* 2009; Xu and Zhang, 2009; Nair *et al.,* 2011). Further, TiO_2 also generally has relatively low of surface area which influencing the adsorption the organic pollutant on the surface particle and also reduce photocatalytic activity (Ta-Tang *et al.,* 2012).

Some works are developed to overcome the disadvantages of pure TiO_2 such as mixed-phase of TiO_2, which includes anatase–rutile, anatase–brookite, brookite–rutile, and anatase–TiO_2 (B) (Meulen et al., 2007; Li *et al.,* 2008; Scotti *et al.,* 2008; Li and Liu, 2009; Zheng *et al.,* 2010). One of the TiO_2 mixed phase is Degussa P25 material, which consists of 80% anatase and 20% rutile. This material exhibits higher photocatalytic activity than its pure-phase of TiO_2.

To enhance the photocatalytic activity of TiO_2 can also be done by some modification such as TiO_2 doping with other metal or noble metal (Chen and Mao, 2007); Zielinska-Jurek *et al.,* 2011; Yu *et al.,* 2011). Another is immobilization of TiO_2 over support materials which have high surface areas, such as activated carbon, zeolite, silica, and Al_2O_3 (Wang *et al.,* 2009; Tayade *et al.,* 2007; Pucher *at al.,* 2007; Chen *et al.,* 2005). By using this method, the surface area as important factor influencing adsorption rate and photocatalytic efficiency, will increase significantly. Then the surface area determines pre-adsorbed pollutant molecules on TiO_2 particles facilitate degradation (Yu *et al.,* 2011). Some researchers also report that ZnO which has band gap of 3.2 eV is an effective catalyst in oxidation of dyes, phenolic compound and also on the treatment of groundwater pollutant (Villasenbor *et al.,* 1998; Akyol *et al.,* 2004; Khodja *et al.,* 2001). Further, in another recent study, Al_2O_3 was also found to be a sensitive photocatalyst under UV illumination (Fa-Tang *et al.,* 2012).

A further development is reported that the addition of small amounts of oxidants such as hydrogen peroxide result in the more perfectly of the active hydroxyl radicals formation. The combination of oxidants and photocatalyst will have an excellent performance in removal of highly refractory compounds. In addition to hydrogen peroxide and ozone, the other oxidants which are widely studied are peroxymonosulfate (PMS). The PMS which can be generated as sulfate radical by UV or catalyst has lot of interest due to the high of its redox potential. Several studies have reported about the use of sulfate radical in the photocatalytic oxidation of organic contaminant in wastewater in the present of TiO_2 and UV-light radiation (Khalil *et al.,* 1998; Yang *et al.,* 2008; Fujishima *et al.,* 1981; Bekbolet and Balcioglu, 1996; Matthews and McEvoy, 1992). This research conducted photocatalytic oxidation of phenol by using photocatalyst of Ru impregnated TiO_2 and Al_2O_3 in the present of PMS as oxidant and UV-light.

Materials and Methods

Experimental setup of photocatalytic oxidation

The photocatalytic experiment is run in a 1 liter double jacket reactor which placed in UV cupboard with a constant mixing at 400 rpm. The reactor was irradiated with a 500 W (max) of UV-Mercury lamp which is categorized as UV-C, with wave length in range of 200-280 nm from the lamp housing of Oriel 66905 powered by Newport 69911. The radiation temperature was controlled by cooling water which was flowed through an external jacket in the housing lamp. The cooling water was also circulated through the reactor jacket to control reaction temperature. An external tube was dipped in reactor for sample withdrawal at a certain time. The experimental setup sketch can be seen in Fig. 1.

Synthesis of ruthenium catalysts on TiO_2 and Al_2O_3 support

Ru/TiO_2 and Ru/αAl_2O_3 catalyst were synthesized following a general impregnation method. A fix amount of ruthenium chloride (Sigma-Aldrich) was added into 200 mL ultrapure water until the ruthenium compound was dissolved. Next, TiO_2, Degussa P25 [surface area 55.5 m2/g] which obtained from Degussa, Germany was added to the solution and kept stirring for 24 h. The suspension was then evaporated in a rotary evaporator at temperature of 50 ^{0}C under vacuum. Further, the catalyst was recovered and dried in an oven at 120 °C for 6 h. Calcination of the catalyst was conducted in a furnace at 550 °C for 6 h air. Then the catalyst was stored in a desiccator until use. The same method was also conducted to synthesize Ru/αAl_2O_3 (Saputra *et al.,* 2014)

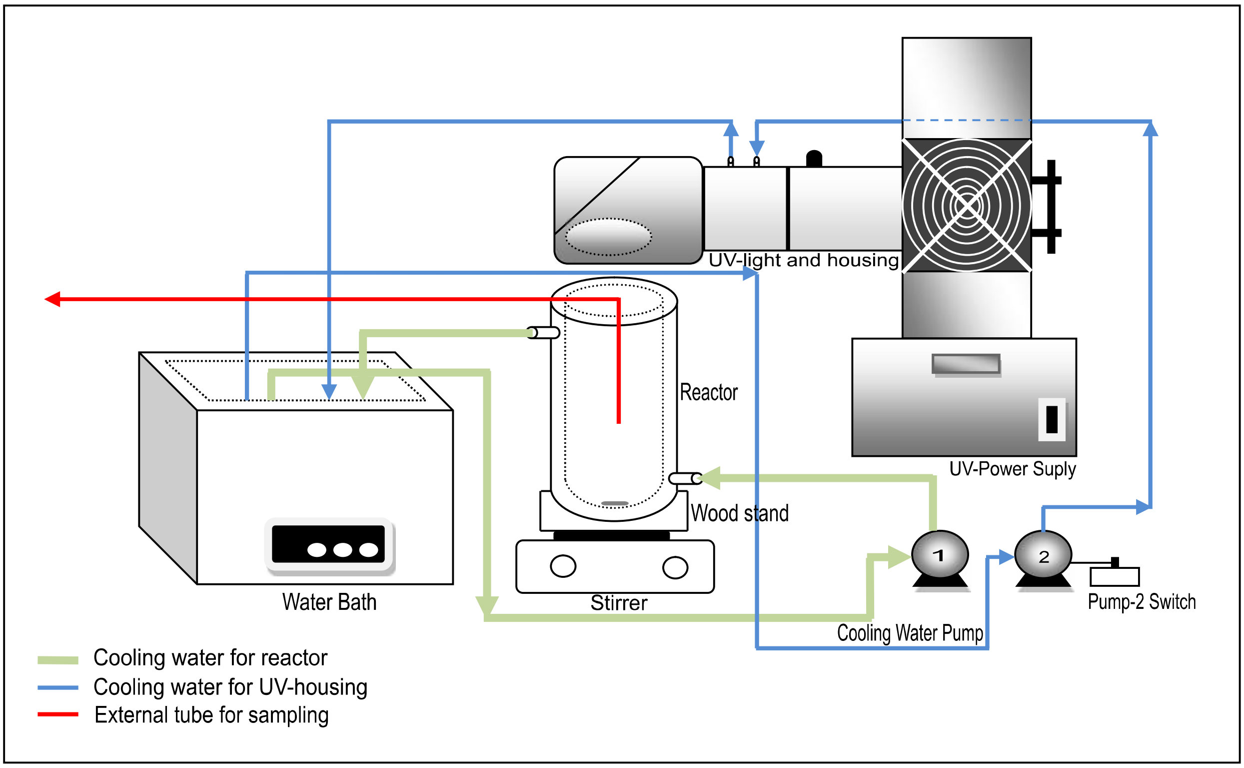

Figure 1. Experimental setup of photocatalytic oxidation

Characterisation of catalysts

Both synthesized catalysts of Ru/TiO_2 and Ru/αAl_2O_3 were characterised by X-ray diffraction (XRD), scanning electron microscopy (SEM) with energy dispersive X-ray spectroscopy (EDS), and N_2 adsorption. The XRD (Siemen, D501 diffractometer) was used to identify the structural features and the mineralogy of the catalysts. The XRD pattern was obtained using filtered Cu Kα radiation with accelerating voltage of 40 kV and current of 30 mA. The samples were scanned at 2θ from 5-100°. Further, to obtain a visual image and identify the texture and morphology of the catalysts, SEM (Philips XL30) with secondary and backscatter electron detectors was used. Energy-dispersive X-ray spectroscopy (EDS) was also used to detect Ru particles on supported catalysts of TiO_2 and Al_2O_3.

Kinetic study of phenol photocatlytic oxidation

Phenol (Aldrich) was used to prepare stock of 5000 ppm. From this stock solution four different concentration of phenol of 25, 50, 75 and 100 ppm were made which were then used in catalytic oxidation of phenol. The solution was stirred constantly at 400 rpm to maintain homogeneous solution. Next, a fixed amount of peroxymonosulphate (Oxone®, DuPont's triple salt $2KHSO_5 \cdot KHSO_4 \cdot K_2SO_4$, Aldrich) was added to the mixture until completely dissolved. Then, a fixed amount of catalysts Ru/TiO_2 or Ru/αAl_2O_3 was added into the reactor. And finally, the power of UV-light which has different power 200, 300 and 500 W was switched on to start the oxidation of phenol. The reaction was run for 1 h and at the fixed time interval, 0.5 mL of a sample was withdrawn from the solution and filtered using HPLC standard filter of 0.45 µm and mixed with 0.5 mL methanol as a quenching reagent to stop the reaction. Phenol was then analysed on a HPLC consisted of isocratic pumps from Varian with a UV-Vis detector at wavelength of 270 nm. The column is C18 with mobile phase of 70% acetonitrile and 30% ultrapure water. Furthermore, the used catalyst were then recycled for multiple round tests, the spent catalyst was recovered after each run from the reaction mixture by filtration and washed thoroughly with distilled water and dried at 70 ^{0}C for reuse.

Results and Discussion

Characterisation of ruthenium impregnated activated carbon and ZSM5 catalysts

The characterization of synthesized catalyst shows that the active metal of Ruthenium has been well dispersed and coated on the support surface of titanium oxide and alumina. The active phase of ruthenium is in form of RuO_2 at XRD 2θ pattern peaks of 28, 35, 40 and 54.3^0 as can be seen in Fig. 2

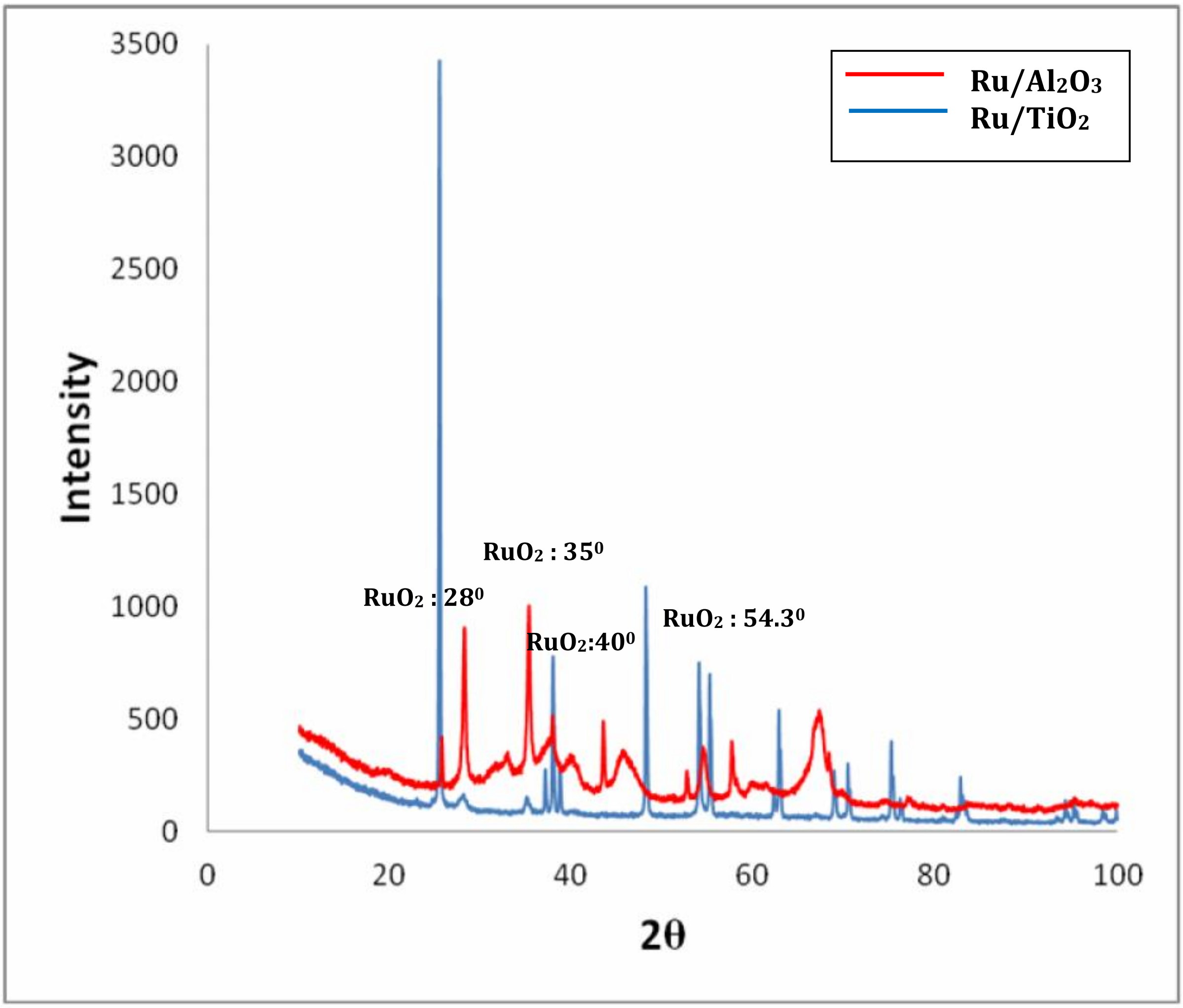

Figure 2. **XRD pattern of Ru/ TiO_2 and Ru/ Al_2O_3**

The presence and dispersion of active metal ruthenium on the support surface were also confirmed by EDS spectra as can be seen in Fig. 3 and Fig. 4. Among five spectrum spot selected, all indicate that there are ruthenium on surface of titanium oxide and alumina.

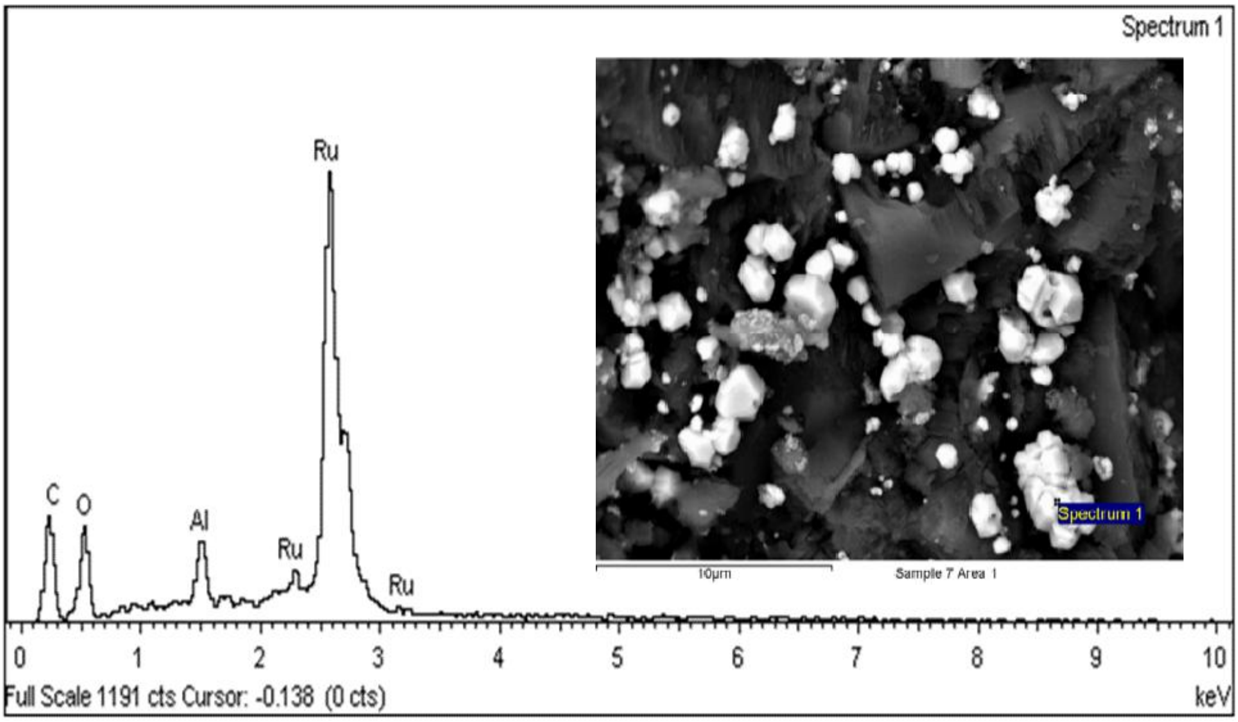

Figure 3. EDS Spectra of Ru/TiO_2

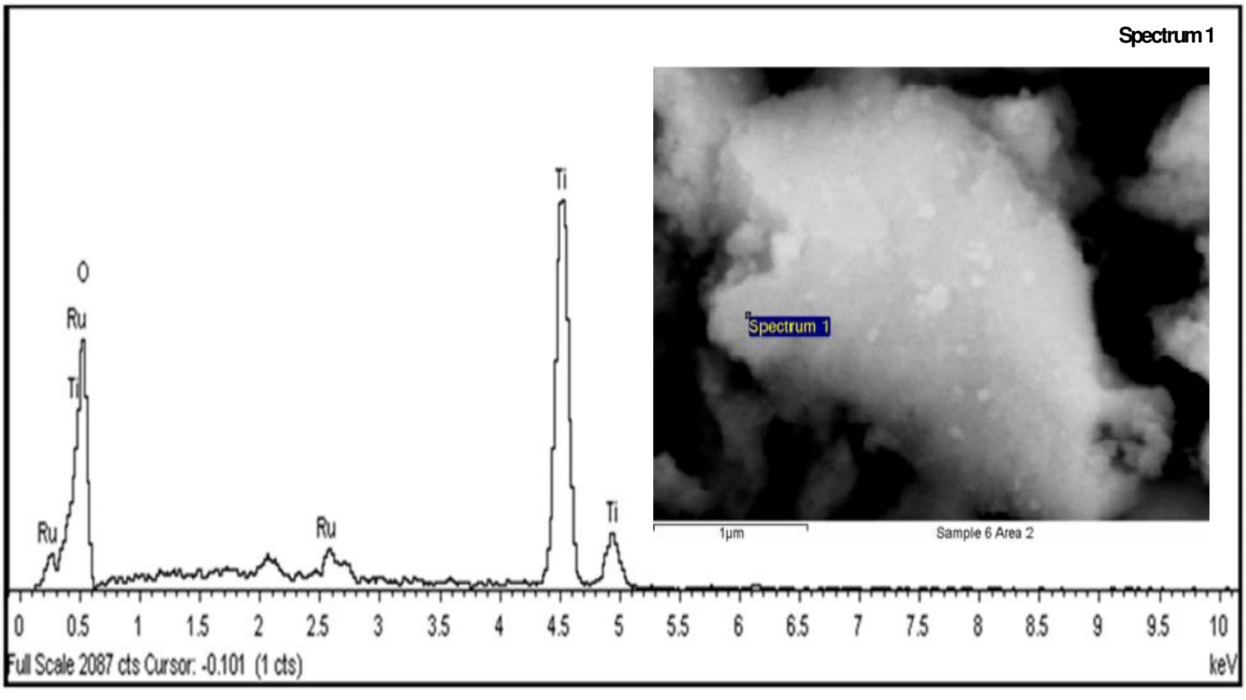

Figure 4. EDS Spectra of Ru/αAl_2O_3

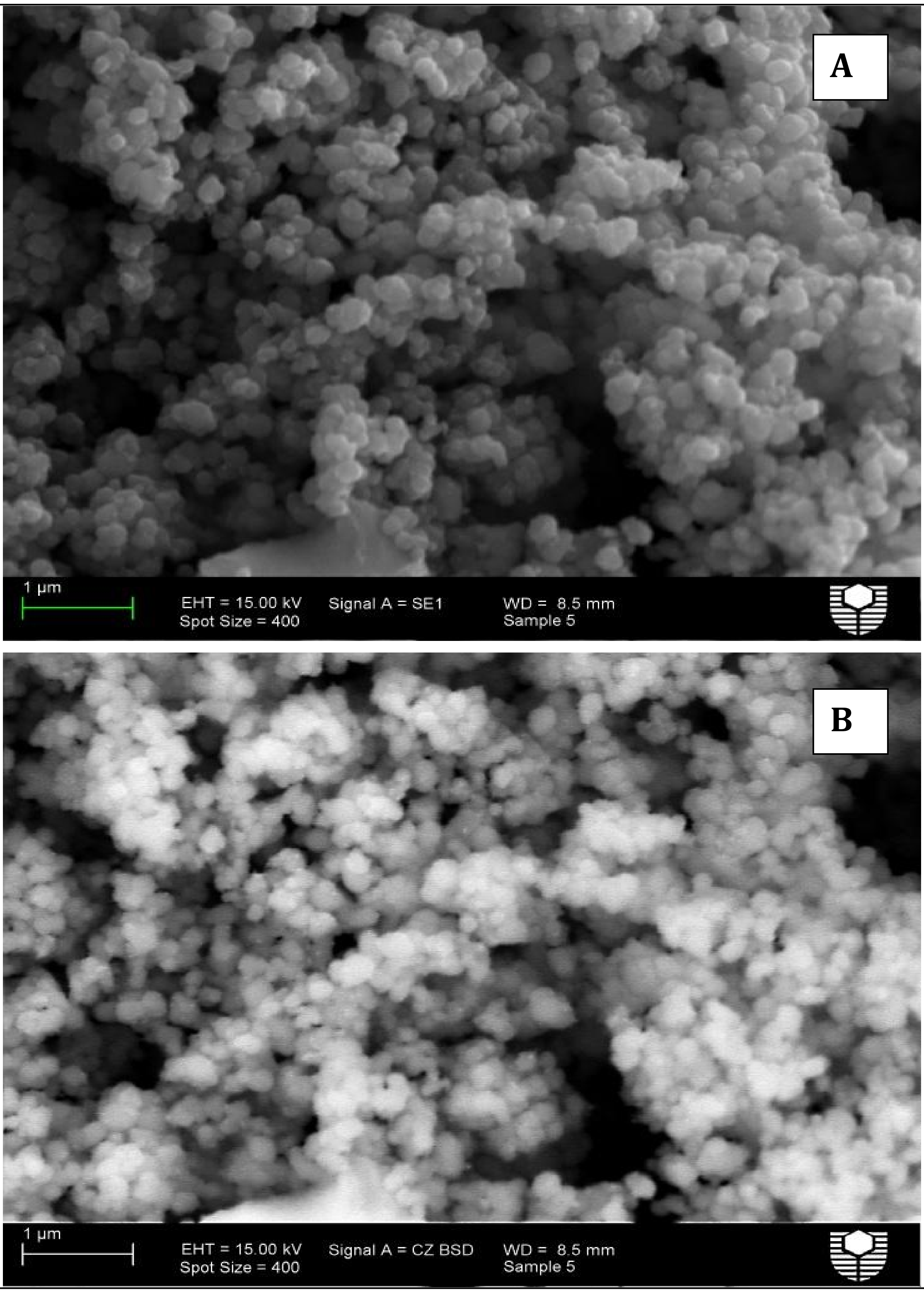

Figure 5. SEM Image of Ru/TiO_2, (A) SE detector, (B) BSD detector

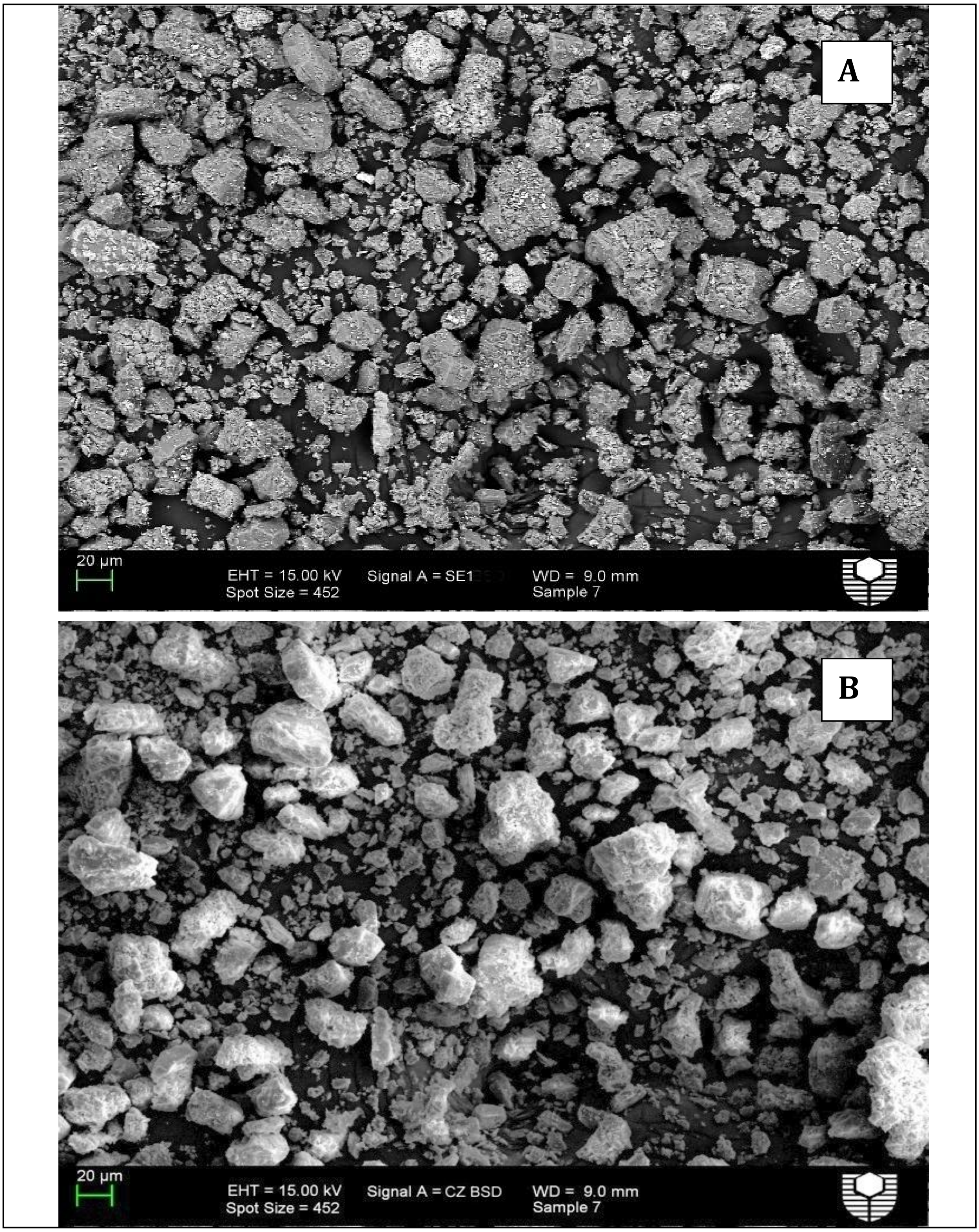

Figure 6. SEM Image of Ru/Al_2O_3, (A) SE detector, (B) BSD detector

Further, SEM images as shown at Fig.5 and 6 describe the morphology of both catalyst of Ru/TiO_2 (Fig.5) and Ru/Al_2O_3 (Fig.6). As seen in the picture, Ru/TiO_2 has much smaller particle size than Ru/Al_2O_3. The presence of ruthenium on the support surface was also analysis by secondary electron detector (SE) and backscattered detector (BSD) of SEM. By using BSD detector at the same area, the presences of ruthenium specks are seen at the brighter area in the catalyst particles. It implies that ruthenium is well coated in the titanium oxide (Fig. 5B) and alumina (Fig. 6B).

Preliminary study of photocatalytic oxidation of phenol

Preliminary tests of photocatalytic oxidation with various samples are shown in Fig. 7. The process was run with reaction conditions of 0.2 g catalyst loading, 1 g of Oxone ® in 500 mL phenol solution of 50 ppm, 25 ^{0}C, stirring speed of 400 rpm and 300 Watt UV-light.
Generally, it is seen that a process involving the catalyst and UV-light give better phenol removal efficiency. As shown in Fig.7, complete removal of phenol by using a combination of catalysts Ru/TiO_2, Oxone and UV reaction can be achieved within 60 minutes. In the same time, photocatalitic oxidation using Ru/Al_2O_3, Oxone and UV (300 Watt) provide about 90% removal efficiency. In can be seen that Ru/TiO_2 slightly better than Ru/Al_2O_3. Another interesting fact is that the phenol removal efficiency can reach 85% by simply using UV and Oxone only. This means that the presence of both catalyst and Ru/Al_2O_3 Ru/TiO_2 in the treatment system only improves phenol removal efficiency in the range of 10-15%. Further, it is also confirmed that UV-light is effective to generate sulfate radical of PMS (Oxone) to degrade phenol as seen in the following Eq. 1.

$$\mathrm{HSO_5^-} + h\nu \rightarrow \mathrm{SO_4^{-\bullet}} + \mathrm{OH^-} \qquad 1$$

$$SO_4^{\bullet -} + C_6H_5OH \rightarrow C_6H_5OH - SO_4^{\bullet -} \xrightarrow{-SO_4^{2-}} C_6H_5OH^{\bullet +} \qquad 2$$

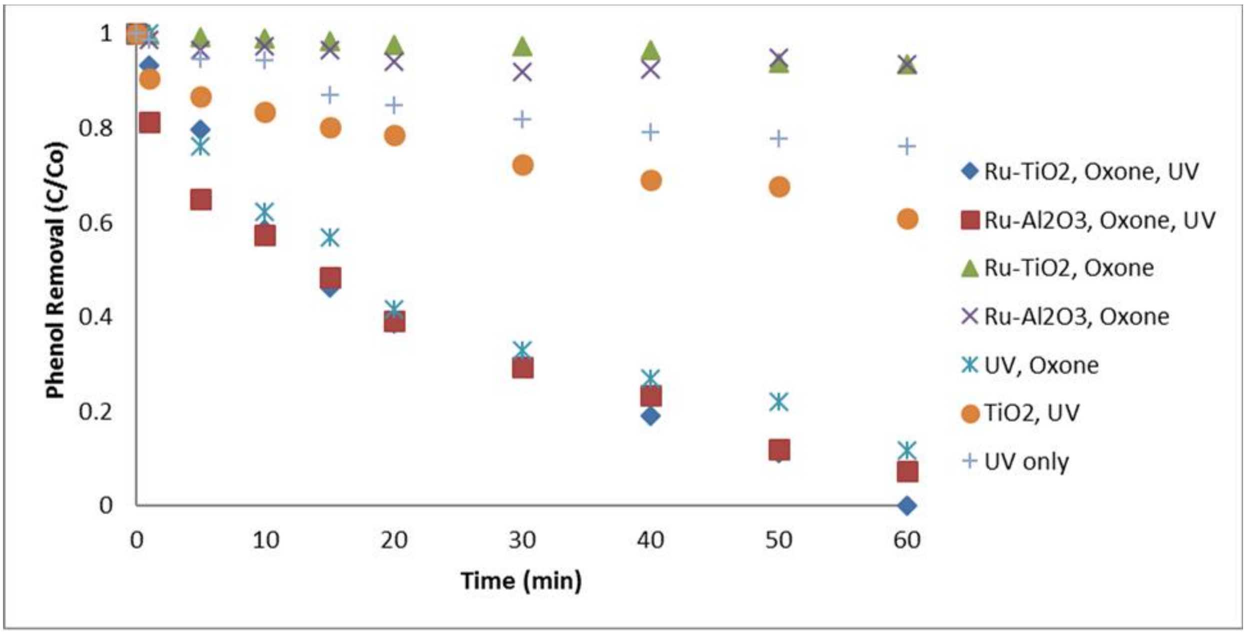

Figure 7. Phenol removal in adsorption and photocatalytic oxidation

On the other hand, the present of photocatalysts of Ru/TiO_2 and Ru/Al_2O_3 give additional acceleration in sulfate radical production in photocatalytic oxidation system. As can be seen from XRD spectra that the main active phase of the catalyst would be RuO_2 therefore, it is believe that the phenol removal mechanism as be presented below.

$$\text{S-Ru(IV)} + \mathrm{HSO_5^-} \rightarrow \text{S-Ru(III)} + \mathrm{SO_5^{-\bullet}} + \mathrm{H^+} \quad \text{(S: solid surface)} \qquad 3$$

$$\text{S-Ru(III)} + \mathrm{HSO_5^-} \rightarrow \text{S-Ru(IV)} + \mathrm{SO_4^{-\bullet}} + \mathrm{OH^-} \qquad 4$$

$$\mathrm{C_6H_5OH} + \mathrm{SO_4^{-\bullet}} \rightarrow \text{several steps} \rightarrow \mathrm{CO_2} + \mathrm{H_2O} \qquad 5$$

Further, the multiple test of the catalyst in phenol removal are presented in Fig. 8. After their regeneration by water washing, both Ru/TiO_2 and Ru/Al_2O_3 catalysts were also tested for multiple uses. It can be seen in Fig. 8 that, both catalysts showed somewhat deactivation in the second and third runs. However, the deactivation was not so significant.

In can be seen from graph the difference of removal efficiency among them is not significantly high. The deactivation occurs presumably due to adsorption of intermediates and a small portion of loose ruthenium leaching from the supports of TiO_2 and Al_2O_3.

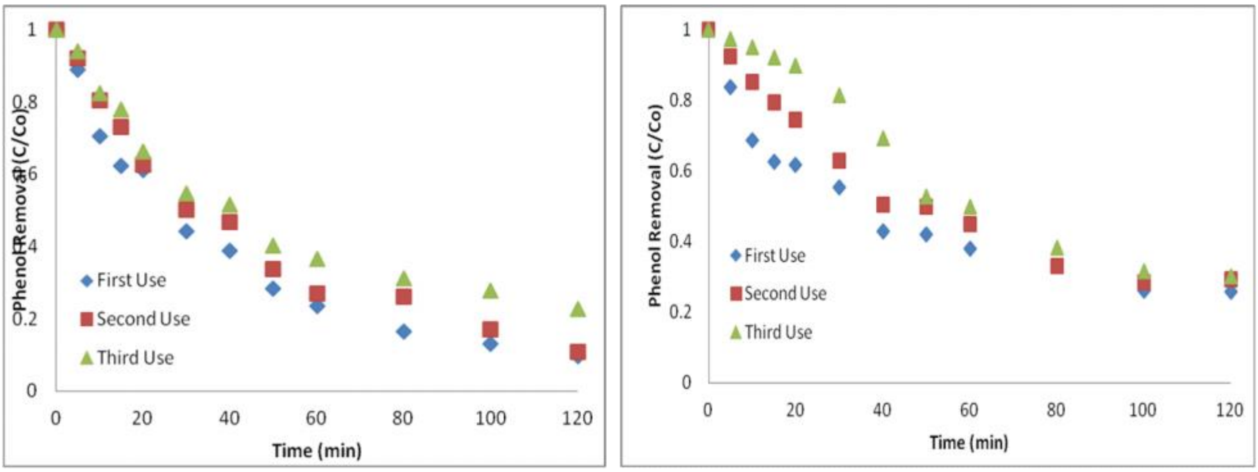

Figure 8. Phenol removal in multiple use of photocatalyst (A) Ru/TiO_2 and (B) Ru/Al_2O_3 at 50 ppm, at 1 g Oxone, 0.2 g catalyst, 25^0C, 200W UV

Effect of UV-light intensity on phenol removal

It is well know that UV radiation is defined as the electromagnetic radiation with wave length range of 10-400 nm. The UV itself consists of V-UV (vacuum UV, 100-200 nm), UV-C (200-280 nm), UV-B (280-320 nm) and UV-A (320-400 nm) as described in Fig.9 [30]. This research used three different UV-light intensity of 200W, 300W and 500W. Among them the 300W power of UV has the optimum result in phenol removal. The UV-light source is come from Mercury Lamp which irradiating the UV-C light with wave length in range of 200-280. This kind of UV is the UV spectral range of interest for the UV photolysis application (Parson and Williams, 2004).

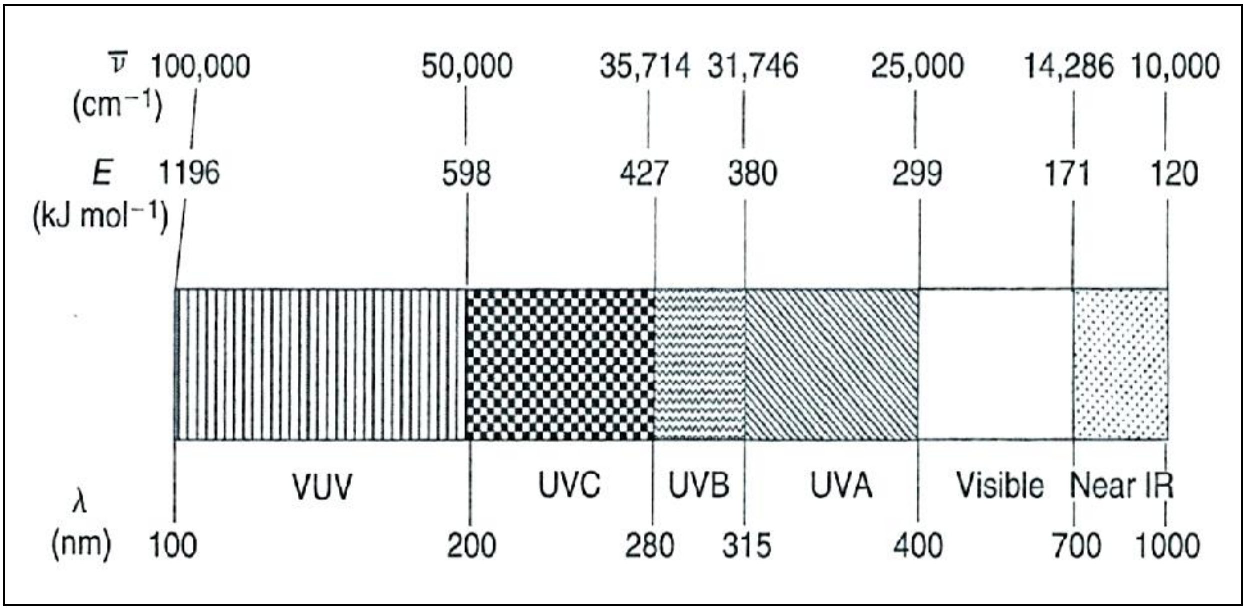

Figure 9. Spectrum of the electromagnetic radiation

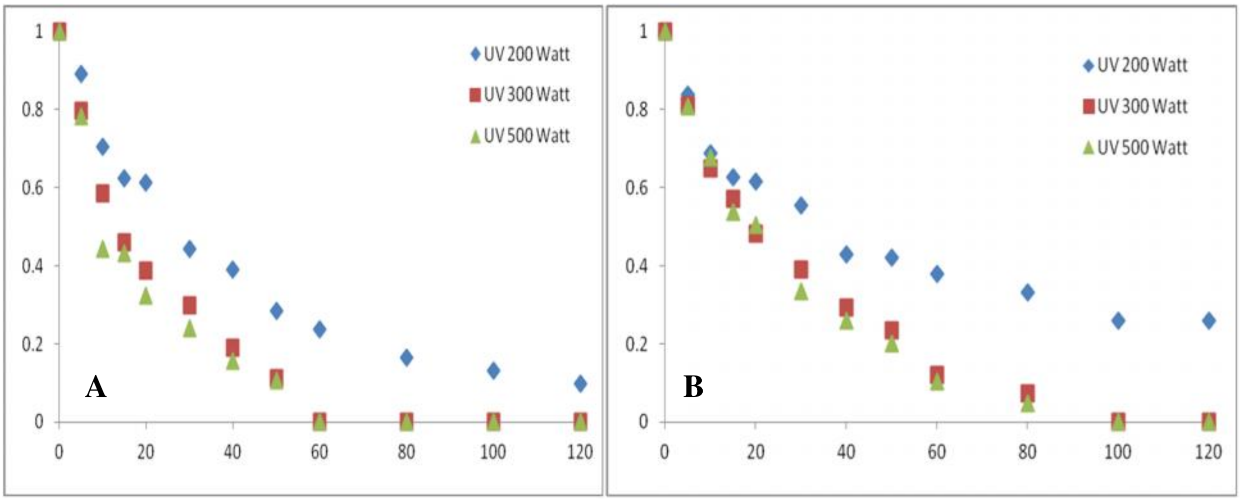

Figure 10. Photocatalytic oxidation of phenol at different UV-light intensity, (A). Ru/TiO_2 catalyst and (B). Ru-Al_2O_3 catalyst.

Further, the effect of UV-light intensity on phenol removal is presented in Fig. 10. As can be seen in Fig. 10A, at 60 minutes reaction time, complete removal of phenol can be reach by using UV power of 300W and 500W while about 75 % of phenol removal by 200W. Similar result is presented in Fig. 10B using Ru/Al_2O_3, complete removal of phenol is reached within 100 minutes at 300W and 500W of UV Power while at 200W, 60% of removal efficiency is obtained.

Effect of reaction parameters on phenol removal

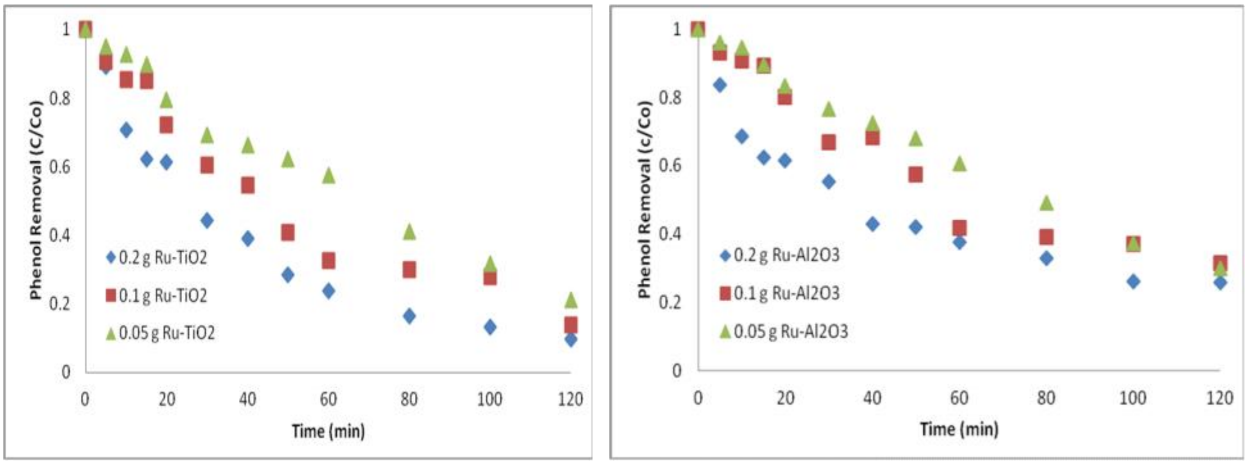

Figure 11. Phenol removal in different catalyst loading (A) Ru/TiO_2 and (B) Ru/Al_2O_3 at 50 ppm, at 1 g Oxone, 25°C, 200W UV

The first parameter is the effect of catalyst loading on phenol degradation. According to Fig. 11, the greater of the amount of catalyst used, the higher of phenol reduction efficiency is. This phenomenon is reasonable, because increasing the amount of catalyst will increase the adsorption and also the availability of catalyst sites to activate oxone. The same trend also occurred with Al_2O_3 in Fig. 11B. For instance, at reaction time of 60 minutes, removal efficiency of 80%, 70% and 40% can be obtained by catalyst loading of 0.2g, 0.1g and 0.05g respectively. However, at 120 minutes, the removal efficiency seems not too significantly change. It is probably due to low amount of remain phenol contaminant in the treatment system. Moreover, the presence of UV-light made removal efficiency increase even some oxidant was added low.

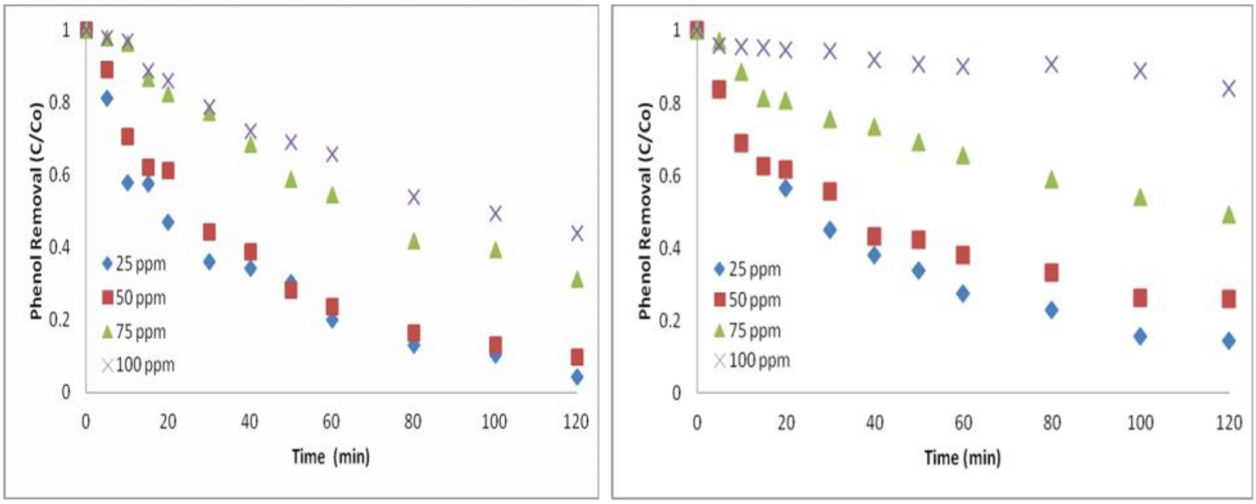

Figure 12. Phenol removal in different concentration (A) Ru/TiO_2 and (B) Ru/Al_2O_3 at 0.2g catalyst, 1 g Oxone, 25^{0}C, 200W UV

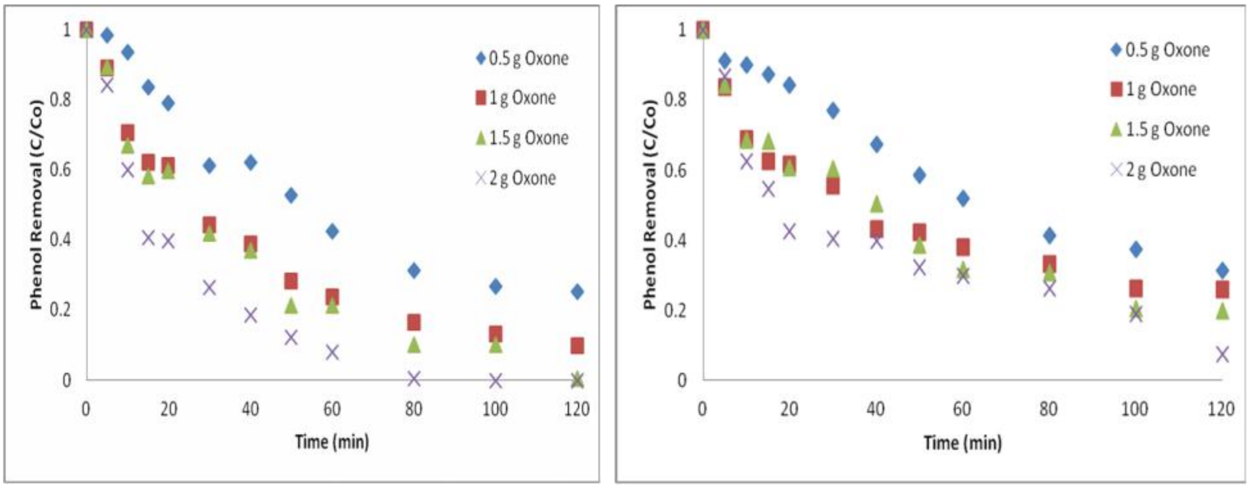

Figure 13. Phenol removal in different Oxone concentration (A) Ru/TiO_2 and (B) Ru/Al_2O_3 at 0.2g catalyst, 1 g Oxone, 25^{0}C, 200W UV

The second parameter measured in this study was phenol concentration in range of 25 - 100 ppm, as shown in Fig. 12. Generally, removal efficiency of phenol decreases with increasing phenol concentration. For instance at 120 minutes as can be seen in Fig. 12A phenol removal efficiency which have concentration of 25 ppm, 50 ppm, 75 ppm and 100 ppm are 95.67%, 90.16%, 68.72% and 55.88% respectively. Similar trend is also found in Fig. 12B using Ru/Al_2O_3.

And the third parameter observed is effect of oxone concentration. Figure 13A (Ru/TiO_2) shows that increased concentration of oxone in a solution will accelerate phenol removal. By using 2g oxone, complete removal can be achieved in about 80 minutes. Similar trend is also observed in Fig. 13B using Ru/Al_2O_3 even with removal efficiency slightly lower than Ru/TiO_2. The increase of reaction rate at the increased oxone concentration is caused by higher production of sulphate radical for reducing phenol.

Phenol photocatalytic oxidation kinetics

Phenol degradation in photocatalytic without an oxidant is occurred with heterogeneous reaction in the catalyst surface. Basically, phenol is directly oxidized on the active hole on catalyst surface. So that intermediate compound is formed and continued with the formation of end product. However, by adding an oxidant such as PMS, the main process will be the formation of sulfate radical which generated by interaction between PMS and the catalyst (Ru/TiO_2 or Ru/Al_2O_3) or caused by interaction between PMS and UV-light. The phenol molecule which initially adsorbed on the catalyst surface then followed by chemical oxidation is fit with the first order kinetics. A general equation of the pseudo first order kinetics can be used, as shown in the following equation.

$$\frac{dC}{dt} = -(k.C) \qquad 6$$

Where *k* is the first order rate constant of phenol removal, *C* is the concentration of phenol at various time, *Co* is the initial concentration of phenol. By integrating the equation above, the profile decrease in phenol concentration can be further elaborated in the following equation.

$$C = Co.e^{-k.t} \qquad 7$$

The Eq. 7 become

$$\text{In}\ (C/C_0) = -k.t \qquad 8$$

The rate constant can be determined by plotting of In(C/C_0) with time, as presented in Fig. 14.

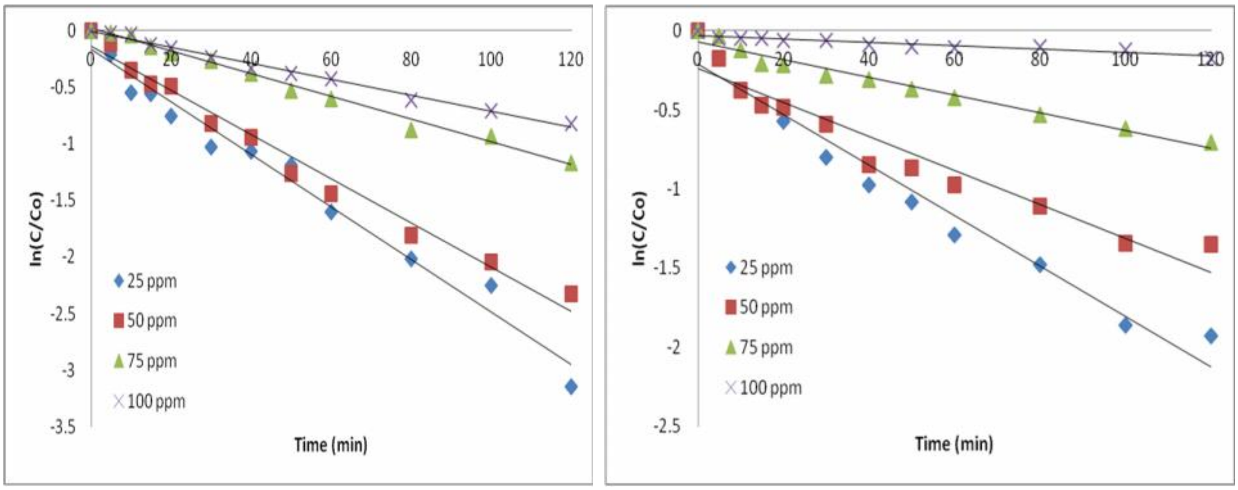

Figure 14. Pseudo first order kinetics (A). Ru/TiO_2 and (B). Ru/Al_2O_3

From data fitting, it is obtained that this reaction can be represented by the pseudo first order kinetics. This can be validated from the values of R^2, which are above 0.9 as shown in Table 1. The calculated rate constants are also presented in Table 1. It is based on an assumption that the process is influenced by several reaction parameters such as oxidant and catalyst concentrations and intensity of incident radiation. The rate constant *(k)* shows that in general the value of *k* for Ru/TiO_2 is higher than Ru/Al_2O_3, which means the Ru/TiO_2 is able to degrade phenol more rapidly than Ru/Al_2O_3.

Table 1. The rate constant at various concentrations of phenol

Catalyst	Phenol Concentration							
	25 ppm		50 ppm		75 ppm		100 ppm	
	k	R^2	*k*	R^2	*k*	R^2	*k*	R^2
Ru/TiO_2	0.0232	0.9767	0.0195	0.9809	0.01	0.9903	0.0071	0.9908
Ru/Al_2O_3	0.016	0.9666	0.0108	0.9255	0.0056	0.9675	0.0011	0.9863

Conclusion

Two photocatalysts of Ru/TiO_2 and Ru/Al_2O_3 catalyst have been successful synthesized using impregnation method followed by calcinations at temperature of 550 ^{0}C. Both catalyst are effective for application of photocatalytic oxidation of phenol in the present of PMS as an oxidan and UV-light. In this study, phenol can be removed within 1 hour from the solution. Activation of PMS for the production of sulphate radicals for phenol degradation is generated by the interaction PMS-Catalyst and PMS-UV. Further, the photocatalyst of Ru/TiO_2 and Ru/Al_2O_3 can increase the phenol removal efficiency of 10-15%. The activity in phenol removal of Ru/TiO_2-PMS-UV is slightly higher than Ru/Al_2O_3-PMS-UV. Both catalysts also showed good performance in the second and third runs after regeneration for multiple uses. The concentration of phenol, catalyst loading and concentration of Oxone® are important parameters that affect the reaction rate in removing phenol. Kinetic studies showed that phenol oxidation on the catalysts, Ru/TiO_2 and Ru/Al_2O_3 in the present of PMS and UV light follows the first order reaction.

References

Akyol A., Yatmaz H.C., Bayramoglu M. (2004). Applied Catalysis B, Environmental. 54 : 19-24.

Bekbolet M., Balcioglu I. (1996). Water Science and Technology. 34: 73-80.

Cong S., Xu Y.M. (2011). Explaining the high photocatalytic activity of a mixed phase TiO2: a combined effect of O2 and crystallinity, J. Phys. Chem. C 115: 21161–21168.

Chen L.C., Tsai F.R., Huang C.M. (2005). Photocatalytic decolorization of methyl orange in aqueous medium of TiO2 and Ag–TiO2 immobilized on _-Al2O3, J. Photochem. Photobiol. A 170 : 7–14

Chen X.B., Mao S.S. (2007). Titanium dioxide nanomaterials: synthesis, properties, modifications, and applications, Chem. Rev. 107 : 2891–2959.

Fa-tang Li , Ye Zhao, Ying-juan Hao, Xiao-jing Wang, Rui-hong Liu, Di-shun Zhao, Dai-mei Chen. (2012). N-doped P25 TiO_2–amorphous Al_2O_3 composites: One-step solution combustion preparation and enhanced visible-light photocatalytic activity, Journal of Hazardous Materials, Vol. 239–240 : 118–127

Fujishima A., Kato T., Maekawa E., Honda K. (1981). Bulletin of the Chemical Society of Japan. 54: 1671-1674.

Grieken R. van., Marugan J., Sordo C., Martinez P., Pablos C. (2009). Photocatalytic inactivation of bacteria in water using suspended and immobilized silver-TiO2, Appl. Catal. B: Environ. 93 : 112–118.

Khalil L.B., Mourad W.E., Rophael M.W. (1998). Applied Catalysis B, Environmental. 17 : 267-273.

Khodja A.A., Sehili T., Pilichowski J.F., Boule P. (2001). Journal of Photochemistry & Photobiology, A: Chemistry. 141: 231-239.

Li G.H., Ciston S., Saponjic Z.V., Chen L., Dimitrijevic N.M., Rajh T., Gray K.A. (2008). Synthesizing mixed-phase TiO2 nanocomposites using a hydrothermal method for photo-oxidation and photoreduction applications, J. Catal. 253 : 105–110.

Li L., Liu C.Y. (2009). Facile synthesis of anatase–brookite mixed-phase N-doped TiO2 nanoparticles with high visible-light photocatalytic activity, Eur. J. Inorg. Chem.: 3727–3733.

Matthews R.W., McEvoy S.R. (1992). Photochem. Photobiol. A : Chem. 64 : 231-246.

Meulen T. van der, Mattson A., Oesterlund L. (2007). A comparative study of the photocatalytic oxidation of propane on anatase, rutile, and mixed-phase anatase–rutile TiO2 nanoparticles: role of surface intermediates, J. Catal. 251:131–144.

Nair R.G., Tripathi A.M., Samdarshi S.K. (2011). Photocatalytic activity of predominantly rutile mixed phase Ag/TiV oxide nanoparticles under visible light irradiation, Energy 36: 3342–3347.

Paola A.D., Garcia-Lopez E., Marci G., Palmisano L. (2012). A survey of photocatalytic materials for environmental remediation, J. Hazard. Mater. 211–212: 3–29.

Parson, S., Williams M. (2004). Advance Oxidation Processes for Water and Wastewater Treatment, IWA Publishing, London.

Pucher P., Benmami M., Azouani R., Krammer G., Chhor K., Bocquet J.F., Kanaev A.V. (2007). Nano-TiO2 sols immobilized on porous silica as new efficient photocatalyst, Appl. Catal. A: Gen. 332: 297–303.

Saputra E., Muhammad S., Sun H., Ang H.M., Tade M.O., Wang S. (2014). Shape-controlled activation of peroxymonosulfate by single crystal α-Mn2O3 for catalytic phenol degradation in aqueous solution, Applied Catalysis B: Environmental, 154-155C : 246-251

Scotti R., Bellobono I.R., Canevali C., Cannas C., Catti M., D’Arienzo M., Musinu A., Polizzi S., Sommariva M., Testino A., Morazzoni F. (2008). Sol–gel pure and mixed-phase titanium dioxide for photocatalytic purposes: relations between phase composition, catalytic activity, and charge-trapped sites, Chem. Mater. 20 : 4051–4061.

Serpone N., Maruthamuthu P., Pichat P., Pelizzetti E., H. Hidaka. (1995). Exploiting the interparticle electron transfer process in the photocatalysed oxidation of phenol, 2-chlorophenol and pentachlorophenol: chemical evidence for electron and hole transfer between coupled semiconductors. Journal of Photochemistry & Photobiology, A: Chemistry, 85(3): 247-255.

Spadavecchia F., Cappelletti G., Ardizzone S., Bianchi C.L., Cappelli S., Oliva C., Scardi P., Leoni M., Fermo P. (2010). Solar photoactivity of nano-N-TiO2 from tertiary amine: role of defects and paramagnetic species, Appl. Catal. B: Environ. 96: 314–322.

Tayade R.J., Kulkarni R.G., Jasra R.V. (2007). Enhanced photocatalytic activity of TiO2-coated NaY and HY zeolites for the degradation of methylene blue in water, Ind. Eng. Chem. Res. 46: 369–376.

Villasenbor J., Reyes P., Pecchi G. (1998). J. Chem. T echnol. Biotechnol. 72: 105-110.

Wang X.J., Liu Y.F., Hu Z.H., Chen Y.J., Liu W., Zhao G.H. (2009). Degradation of methyl orange by composite photocatalysts nano-TiO2 immobilized on activated carbons of different porosities, J. Hazard. Mater. 169: 1061–1067.

Xu H., Zhang L.Z. (2009). Controllable one-pot synthesis and enhanced photocatalytic activity of mixed-phase TiO2 nanocrystals with tunable brookite/rutile ratios, J. Phys. Chem. C 113: 1785–1790.

Yang Q.J., Choi H., Chen Y.J., Dionysiou D.D. (2008). Applied Catalysis B-Environmental. 77: 300-307.

Yu X.X., Liu S.W., Yu J.G. (2011). Superparamagnetic-Fe2O3@SiO2@TiO2 composite microspheres with superior photocatalytic properties, Appl. Catal. B: Environ. 104: 12–20.

Zhang Y.C., Du Z.N., Li K.W., Zhang M., Dionysiou D.D. (2011). High-performancevisible-light-driven SnS2/SnO2 nanocomposite photocatalyst prepared via in situ hydrothermal oxidation of SnS2 nanoparticles, ACS Appl. Mater. Interfaces 3: 1528–1537.

Zheng Z.F., Liu H.W., Ye J.P., Zhao J.C., Waclawik E.R., Zhu H.Y. (2010). Structure and contribution to photocatalytic activity of the interfaces in nano fibers with mixed anatase and TiO2(B) phases, J. Mol. Catal. A: Chem. 316 : 75–82.

Zielinska-Jurek A., Kowalska E., Sobczak J.W., Lisowski W., Ohtani B., Zaleska A. (2011). Preparation and characterization of monometallic (Au) and bimetallic (Ag/Au) modified-titania photocatalysts activated by visible light, Appl. Catal. B: Environ. 101: 504–514.